DOI: https://doi.org/10.15625/0868-3166/22759

Fabrication, and structural instability of a van-der-Waals Fe₅GeTe₂ ferromagnet

T. L. Phan 1,‡ , T. H. Nguyen 2 , H. T. Phuc 3 , N. T. Dang 3 , P. D. Thang 4 , N. H. Tiep 1 and H. N. Nhat 1 ,

E-mail: †ptlong2512@vnu.edu.vn

Received 21 April 2025 Accepted for publication 2 July 2025 Published 11 July 2025

Abstract. This work presents the solid-state reaction method used to fabricate a polycrystalline Fe_5GeTe_2 (FGT) sample, in which chemical reactions of Fe, Ge, and Te precursors took place at $1000\,^{\circ}$ C in a sealed evacuated quartz ampoule. X-ray diffraction analyses indicate the monophase in the rhombohedral $R\overline{3}m$ structure of the as-prepared sample. Unlike ZnO and spinel ferrites, FGT is unstable and easy to decompose to constitute Fe-, Te-, and Ge-related secondary compounds by high-energy ball milling for a short time. Furthermore, the storage of FGT in air at room temperature for a period also leads to its decomposition. Such decompositions would directly influence the magnetic behaviors of FGT. This would limit its application potential in next-generation electronic and spintronic devices.

Keywords: Van-der-Waals 2D materials; Fe₅GeTe₂; structural instability.

Classification numbers: 75.50.Pp; 61.05.cp; 68.37.Hk; 74.25.Ha.

1. Introduction

Semiconductor technology has continuously developed. With necessitous demands on reducing the size of electronic devices for increasingly sophisticated applications, the size of ICs/chips becomes smaller and smaller, while the integration density of transistors in these ICs

¹Faculty of Engineering Physics and Nanotechnology, VNU University of Engineering and Technology, 144 Xuan Thuy, Cau Giay, Hanoi, Vietnam

²Department of Physics, Nha Trang University, Nha Trang, 650000, Vietnam

³Institute of Research and Development, Faculty of Environmental and Natural Sciences, Duy Tan University, Da Nang, Vietnam

⁴Faculty of Physics, VNU Hanoi University of Science, 334 Nguyen Trai, Thanh Xuan, Hanoi, Vietnam

constantly increases. These have remarkably reduced the circuit size in ICs. Until now, the circuit size has been reduced to ~3 nm. It is expected to go down below 1 nm by 2035 [1]. Unlike conventional physical rules, the quantum effects occurring in nano-sized ICs influence the operation and stability of electronic devices, which could end the Moore law. In the face of such challenges, one has paid attention to the use of the electron's spin. An electronic device employing both electron's charge and spin behaviors is defined as *spintronics* [2]. To realize this idea, it is necessary to fabricate ferromagnetic-semiconductor-based electronics, in which a spin-polarized current coexists together with the current of charge carriers. Though ferromagnetic semiconductors have been successfully fabricated, creating a spin-polarized current integrated into conventional electronic devices is still problematic, particularly the challenges related to the interfacial region among hetero-structured materials due to lattice defects and strain [3,4].

The discovery of graphene in 2004 and the 2010 Nobel Prize in Physics [5] have rapidly attracted intensive interest from the scientific and technological community. Basically, graphene is a two-dimensional (2D) monolayer material that can be exfoliated from a graphite structure. Graphite-like 2D materials have weak electrostatic interaction between layers characterized by the van der Waals (vdWs) force. An interesting point for vdWs materials is the possibility of exfoliating them into a monolayer or multilayer, enabling precise control over the thickness and, consequently, the emergence of novel physical properties that are absent in conventional materials. For non-magnetic vdWs materials, magnetic ordering can be established upon doping the 3d-4f element, changing the number of monolayers, and/or applying an external electric field [6]. Using this materials generation, the problems related to interfacial layers and lattice strain can be solved. Additionally, lattice misfits between layers are also new factors that could be used to control the physical properties. It has been believed that the integration of multiple-ordering states in vdWs materials would lead to the birth of new 2D/vdWs-based spintronic devices and continuously extend the Moore law [7]. These devices can be applied to emerging technologies, such as 5G/6G networks, the Internet of Things (IoT), artificial intelligence (AI), neuromorphic computing, and so forth [8–10].

Among vdWs-type materials, Fe_nGeTe_2 (n is an integer number changing from 3 to 7) has been recommended to be itinerant ferromagnets with high T_C values (T_C is defined as the Curie temperature), which are potential candidates for spintronics [11, 12]. Under standard atmospheric conditions, it is hard to synthesize these monophase materials. They are usually fabricated under vacuum and high-temperature conditions. Depending on n, ferromagnetic ordering can exist above 500 K [13]. It has been found that Fe_nGeTe_2 -based heterostructures exhibit the magnetoresistance (MR) effect, in which MR magnitude is strongly dependent on the thickness of heterostructure layers [14]. Though many works on magnetic, magnetoelectric, and Skyrmionic behaviors of Fe_nGeTe_2 have been done [14–16], there are fewer investigations on their structural stability. More recently, Guo *et al.* [17] have performed first-principles calculations and found a prone oxidation of Fe_nGeTe_2 in ambient air. Some experimental evidence also indicated the natural oxidation process of Fe_3GeTe_2 -related films as being exposed to air [18, 19]. To get more insight into this material system, we consider the stability of a bulk Fe_5GeTe_2 sample under the impacts of the mechanical milling and the long-term storage in normal air conditions.

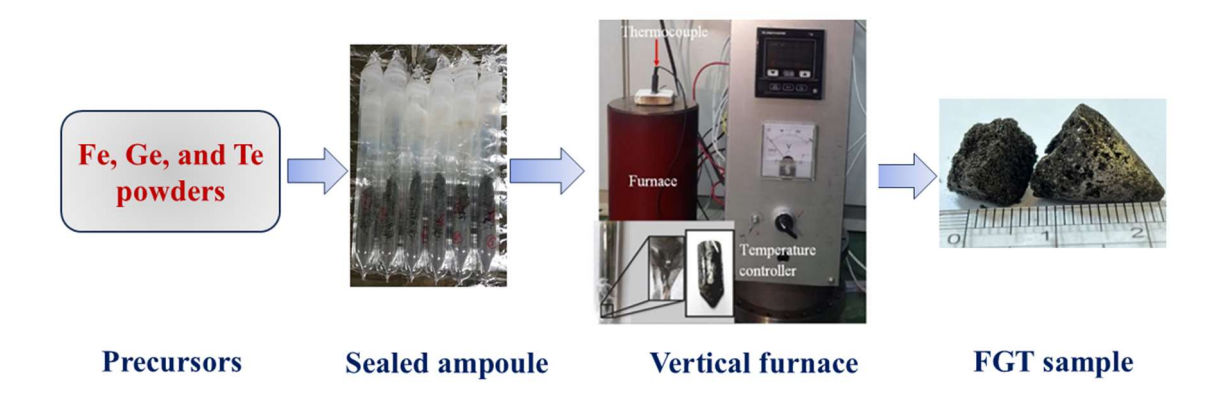


Fig. 1. A sketch diagram of FGT fabrication processes based on the ceramic method.

2. Experiment

Herein, the typical material of Fe₅GeTe₂ (FGT) has been selected for fabrication and investigation. First, high-purity Fe, Ge, and Te powders with the molar ratio of 5:1:2 (Fe:Ge:Te) were scaled and well mixed. The blend was poured into a quartz tube, which was then evacuated and sealed. To mitigate the risk of oxidization caused by potential breakage of the inner ampoule due to mismatched thermal expansion coefficients, the sealed ampoule was placed within a larger quartz ampoule for additional protection. This system was placed in a vertical electric furnace, and then its temperature was gradually increased to 1000 °C at a rate of 50 °C/h. After maintaining 1000 °C for 10 h, the furnace would be cooled slowly to room temperature. Necessary steps to fabricate FGT are shown in Figure 1. The obtained cooled sample was checked for its particle morphology and surface elemental identity by using an electron scanning microscope equipped with energy-dispersive X-ray spectroscopy (EDS). Its crystal structure was examined by an X-ray diffractometer (Bruker, D8 Discover) working with a Cu- K_{α} radiation source. To check the stability of the crystalline structure, a part of the sample was carried out by mechanical-ball grinding by using an 8000D mixer/mill, and the zirconia grinding media (consisting of a vial, 45 ml, containing balls of ~12.5-mm diameter) supplied by SPEX SamplePrep. Milling processes were carried out in an Ar atmosphere at different times. Another part was stored in normal air conditions at room temperature. After several months, its crystal structure was also rechecked by an X-ray diffractometer. Magnetic behaviors of typical samples were selected to study upon temperature- and magnetic-field-dependent magnetization measurements, using a vibrating sample magnetometer (VSM, Lakeshore).

3. Results and discussion

After fabrication, the obtained FGT sample is in the solid bulk and has a neutral grey, which consists of small particles with shiny faces similar to anthracite. Its powder XRD data shown in Figure 2(a) indicate narrow diffraction peaks. Its pattern features are fairly similar to those of Co-doped FGT samples [20]. A detailed analysis using Rietveld refinement has proved FGT crystallizing in the rhombohedral structure, belonging to the $R\overline{3}m$ space group, with a lattice parameter $a = b \approx 4.02$ Å and $c \approx 29.30$ Å. Besides the addressed strong (00*l*)-type Miller indices, there is

a weak-intensity peak beside the (009) peak, which is assigned to the (104) plane. Apart from the mentioned peaks, no extra peaks have been detected, to the limit of the used X-ray diffractometer. These features reflect the polycrystalline behavior and dominant vdWs-type layer-by-layer structure of the fabricated FGT sample. It has been known that the FGT structure is constituted from an ABC-stacking of vdWs slices. Each slice contains Fe and Ge atoms sandwiched between Te atomic layers. A given slice consists of three Fe sites, namely Fe1, Fe2, and Fe3, as illustrated in Fig. 2(b) [21]. While Fe2 and Fe3 sites are almost unchanged, Fe1 sites are usually influenced by fabrication conditions [21,22].

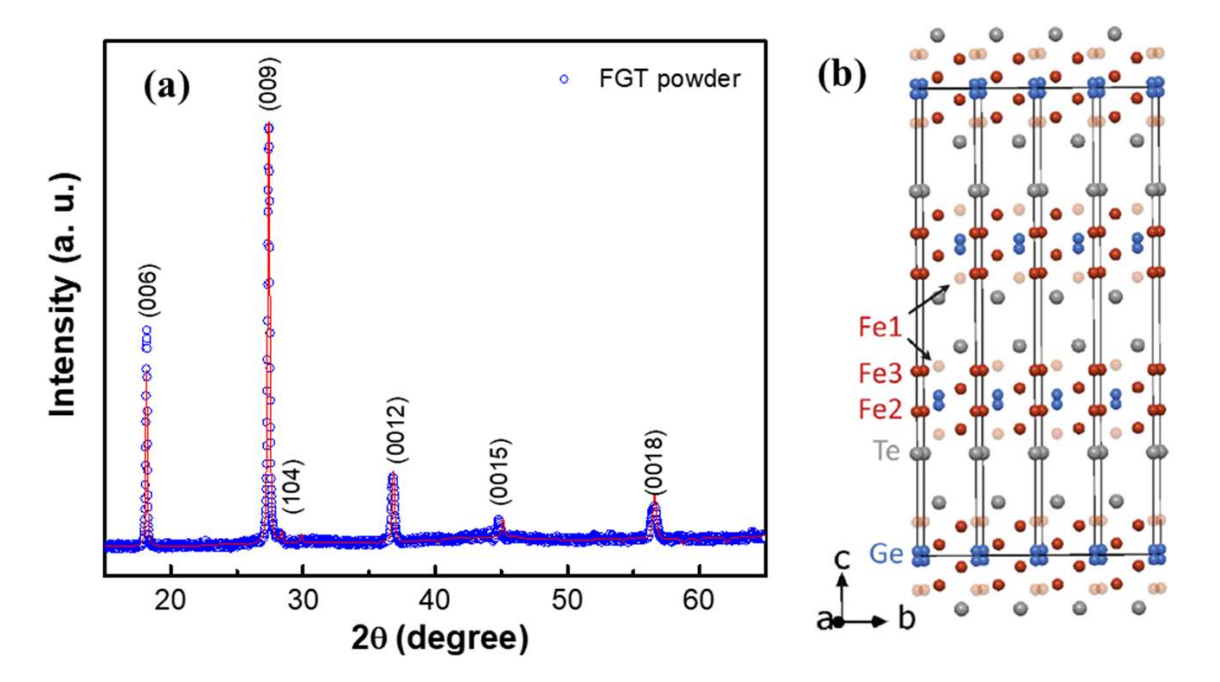


Fig. 2. (a) XRD data (circle symbols) of the as-prepared FGT sample fitted to the $R\overline{3}m$ rhombohedral-structure model (the solid line) based on Rietveld refinement, and (b) its 3D crystal structure for illustration [21].

Having checked the particle morphology by means of a field-emission scanning electron microscope (SEM), we have found FGT constituted from microparticles. Their size ranges from 2 to ~10 μ m, as shown in Figure 3(a, b). Without Pt coating, it is still easy to record clear SEM images of FGT. This is due to its metallic/itinerant behavior [23]. During the particle-morphology investigation, we have also recorded an EDS spectrum for a selected area of ~100 μ m². The spectrum graphed in Fig. 3(c) indicates the presence of Te, Fe, and Ge elements without impurity. Spatial distributions of these elements in the FGT sample are homogeneous, as seen from the element mapping images, Fig. 4(a-c). The EDS analysis determined the chemical components of Fe, Ge, and Te in weight percentage to be about 45.71, 12.08, and 42.21%, respectively.

The above investigations have demonstrated the monophase and crystalline quality of the as-prepared FGT. To study the influence of the grinding time (t_m) on its structural characterization,

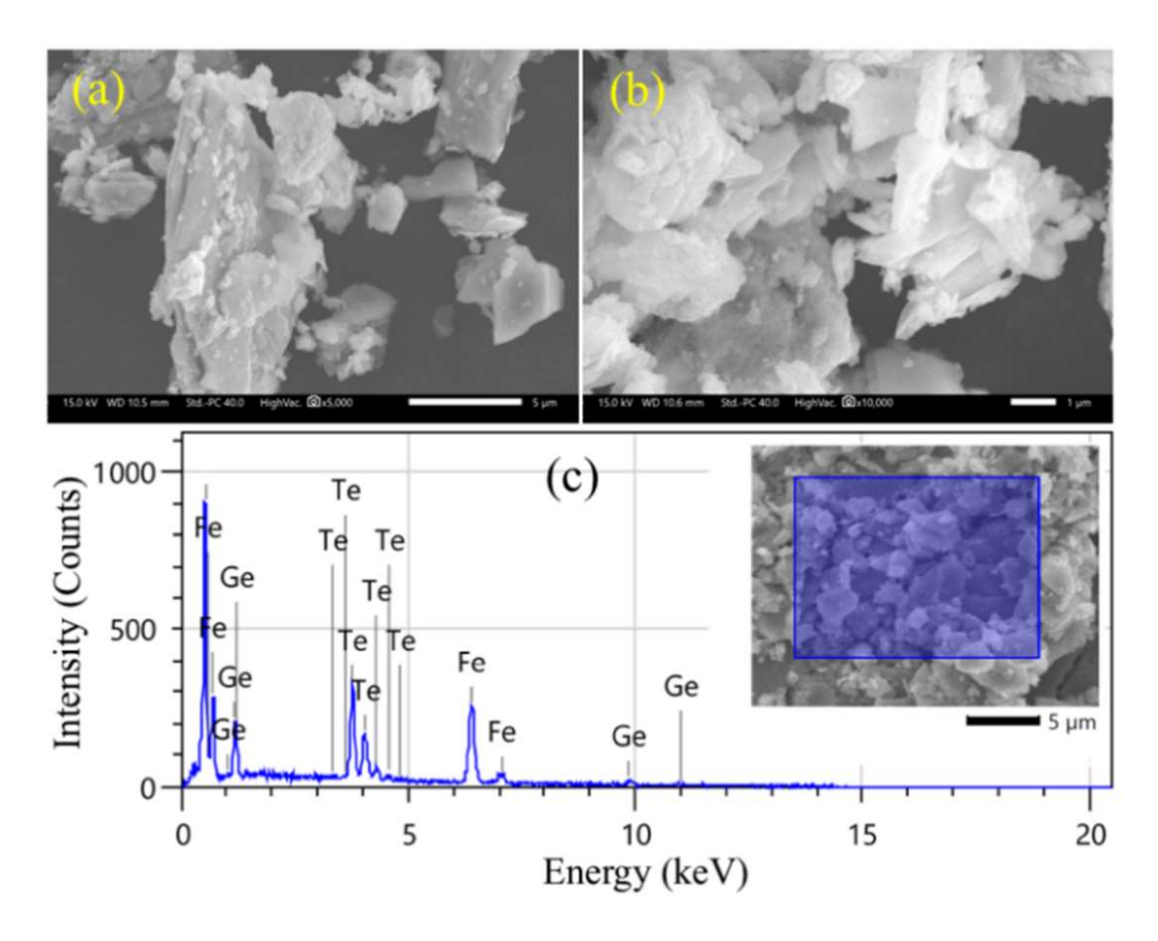


Fig. 3. SEM images recorded with different scale bars of (a) 5 μ m and (b) 1 μ m, and (c) EDS spectrum of FGT (the inset shows a selected area used to record EDS data).

an amount of FGT in powder was poured into the grinding media with the ball-to-powder ratio of 3:1. The grinding was performed in an argon ambiance for various t_m values. As changing t_m , XRD data obtained from the ground samples indicate an instability of FGT, as seen in Figure 5(a). FGT is easily demolished after a short grinding time. Specifically, an increase of t_m from 20 s to 10 min results in an appearance of extra diffraction peaks at about 26.5, 28.4, 30.3, 43.1, 43.8, and 46.7°. They appeared just after grinding for 20 s and became more visible as increasing t_m . Among these, the peak at ~28.4 is assigned to the (104) plane, while that at ~30.3° could be related to the (015) plane of the $R\bar{3}m$ rhombohedral structure of FGT. Together with the strong (00l)-indexed peaks, these (104) and (015) peaks are also addressed as the solid lines in Figure 5(a). Such features reflect that the grinding process caused the random orientation and structural disorder of FGT crystals. The other peaks addressed as the dotted lines in Figure 5(a) are from secondary phases. According to references, rectangle-labeled peaks at about 43.1 and 43.8° are related to GeTe (GT) [24]. The peak at ~26.5° could be attributed to Ge [25] while the others at ~30.3 and 46.7° (denoted as asterisks) could be from FeTe₂ and/or FeTe (FT) [26, 27]. The increase of t_m leads to the widening of all characteristic XRD peaks of FGT owing to the particle-size reduction.

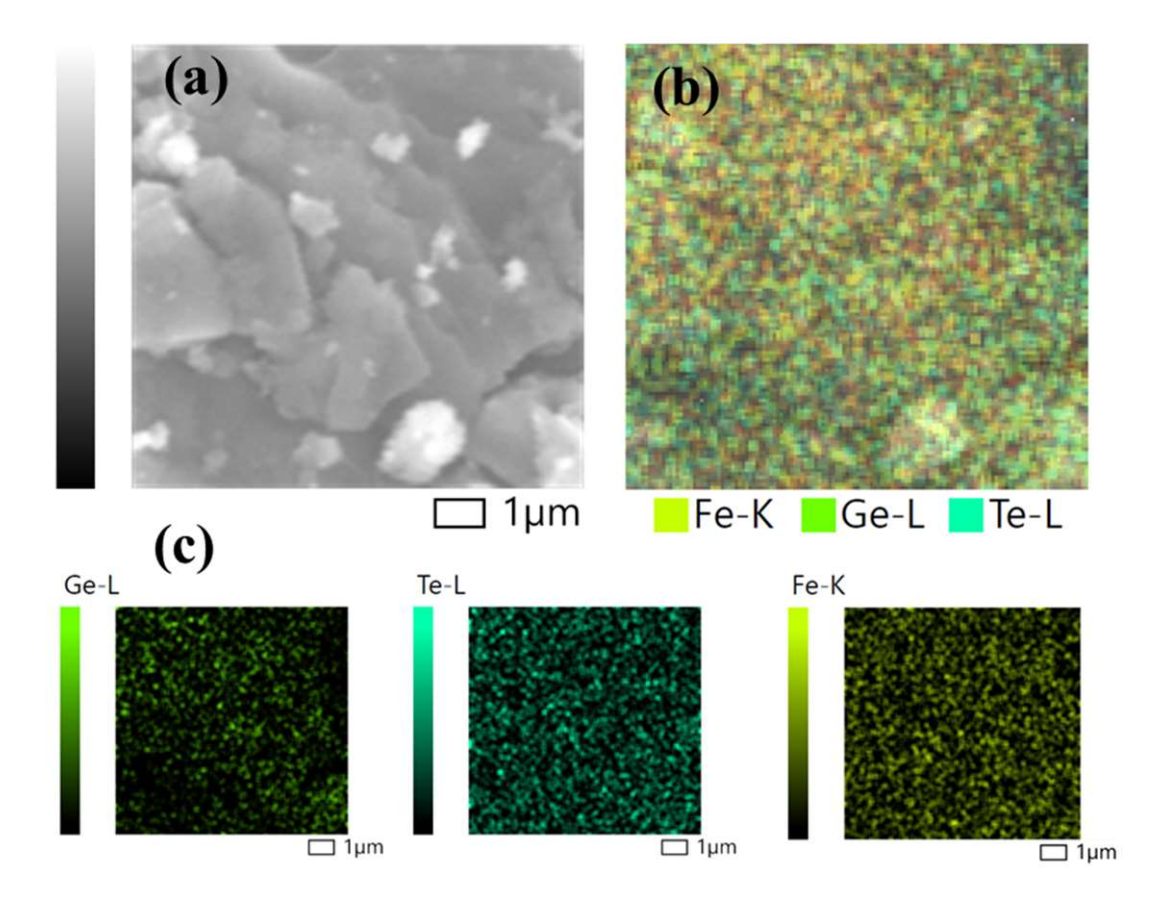


Fig. 4. (a) A sample area selected to record the spatial distribution of (b) all three elements as indicated, and (c) individual Ge, Te and Fe maps.

However, no XRD peak associated with the ZrO_2 grinding media has been recorded, indicating the purity of fabricated samples.

Due to strong ball-ball and ball-vial-wall collisions taking place in the grinding process, we think that FGT particles were fragmented and locally heated. Under thermal-energy impacts (the local heating), FGT could be partially decomposed to form Ge, GeTe, FeTe₂, and/or FeTe compounds, as discussed. Unlike FGT, crystal structures of ZnO, and CoFe₂O₄ spinel ferrites are really stable by high-energy ball milling [28, 29]. The milling just changes their particle size and physical properties.

Surprisingly, when FGT is kept in normal air conditions at room temperature (without controlling humidity, oxygen, light, and so forth) for about one and three months, the XRD features of these samples become different from the XRD data of the as-prepared and ball-ground FGT samples; see Figure 5(b). Apart from the peaks as addressed above, there are additional ones, typically peaking at ~22.6, 41.1, and 49.5° (marked as the dashed lines and circumflexes in Figure 5(b)). Their accurate origin is not easy to identify because many possible secondary compositions could be constituted. As discussed by Guo and Xie *et al.* [17, 18], oxygen, carbon dioxide,

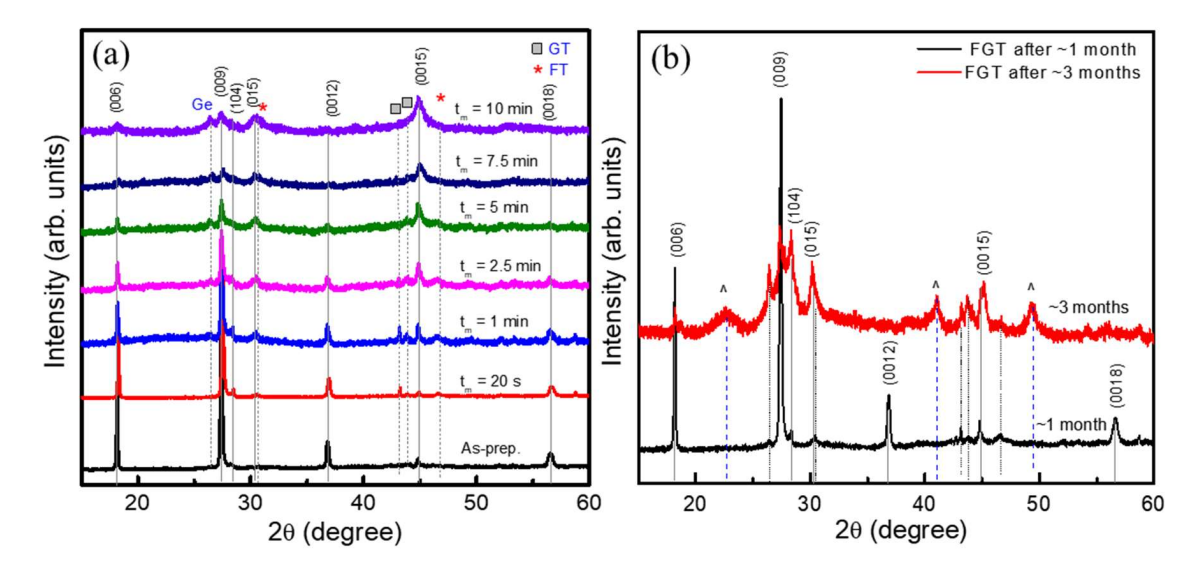


Fig. 5. XRD patterns of (a) milled FGT samples varying as a function of t_m , and (b) of FGT stored in normal air conditions (Northern Vietnam) after about one and three months. Herein, the solid and dotted/dashed lines are assigned to the diffraction peaks of the $R\overline{3}m$ rhombohedral FGT and secondary phases, respectively.

and so forth in air could also penetrate the layer-by-layer structure and cause oxidization of FTG. These processes would lead to the formation of Fe-, Ge-, and/or Te-related secondary compounds. Decomposition mechanisms of FGT could be similar to those proposed for Fe₃GeTe₂ [18].

The above results reflect the structural instability of FGT when it was reduced to the nanometer size by ball grinding and exposed to air for long-term storage (i.e., FGT would be degraded). This also demonstrates the difficulty in fabricating, storing, and applying FGT for microelectronic technology, particularly for its nanostructures. Similar to FGT, many research works have also found the instability of other vdWs-type materials, such as Fe₃GeTe₂ [18], Fe_{3-x}GeTe₂ [19], Cr₂Ge₂Te₆ [17], and FeSe [30]. To protect such air-sensitive vdWs-/2D-type materials, capping/decapping technology has been studied and developed [31,32].

Herein, we have also used a VSM to check the magnetic properties of two typical samples: the as-prepared and ~3-months-stored FGT samples, in which the latter is noted as the aged sample. Temperature-dependent magnetization, M(T), measurements of these samples were carried out in an applied field H = 1 kOe under the field-cooled condition. For the as-prepared FGT, its M(T) data shown in Fig. 6(a) indicate that M gradually tends to decrease when T increases from 200 K to ~270 K. An increase of T to higher values would reduce M rapidly, due to the decline of magnetic ordering by thermal energy. If performing the dM(T)/dT curve, Figure 6(b), we have determined the ferromagnetic-paramagnetic transition temperature (T_C) from its minima, which is about 280 K. This value is in good agreement with the T_C range (270~310 K) reported in the literature [16, 33]. At temperatures $T > T_C$, M gradually decreases to zero. However, M(T) features of the aged sample differ from those of the as-prepared FGT; see Figure 6(a). Its M in the ferromagnetic region decreases remarkably, while its T_C (~286 K) is about 6 K higher than the T_C

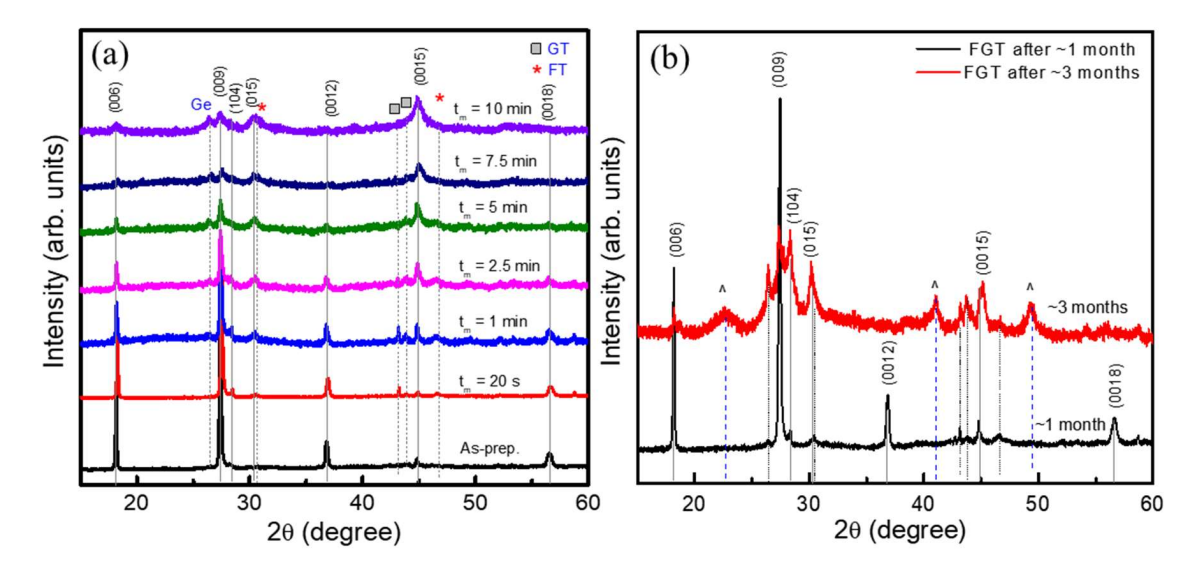


Fig. 6. (a) M(T) and (b) dM(T)/dT curves of as-prepared and aged FGT samples at H = 1 kOe for comparison, and (c) M(H) loops of these two samples recorded at 250 K.

value of the as-prepared sample, Figure 6(b). Additionally, above T_C , its background signals are more stable and higher than those of the as-prepared FGT. These background signals are ascribed to Fe-based magnetic phases, such as FeTe₂ ($T_C > 400 \text{ K}$) [34] and/or Fe₃O₄ ($T_C > 800 \text{ K}$) [35], that could be formed during the FGT decomposition in air. Meanwhile, the T_C increase of the aged sample could be associated with the formation of Fe-rich regions that enhance ferromagnetic interactions between Fe ions at the Fe1, Fe2, and Fe3 sites. If considering M(H) hysteresis loops recorded at 250 K in the ferromagnetic phase, Figure 7(c), one can see the soft behavior of both samples, with coercive force values of ~70 Oe. Similar to M(T) data in the ferromagnetic region, M of the aged sample was decreased in comparison to that of the as-prepared one. This decrease of M is related to the appearance of secondary phases, such as non-magnetic Ge [36], and so forth, which diluted the ferromagnetic phase of FGT. Clearly, such structural and magnetic instabilities of FGT would limit its applicability in electronic and spintronic devices.

4. Conclusion

We used the ceramic method to prepare a polycrystalline FGT sample. The preparation was carried out in an evacuated quartz ampoule. After XRD analysis indicated that the as-prepared FGT has the $R\overline{3}m$ rhombohedral monophase, with the vdWs-type layer-by-layer structure. By reducing the particle size to the nanoscale upon high-energy ball grinding, we have found the instability of FGT. It is easy to partially decompose to Fe-, Ge-, and Te-related compounds, even for a short grinding time - just 20 s. Additionally, by storing FGT in normal air conditions at room temperature for about one to three months, FGT would also be partially decomposed. Such structural changes remarkably impacted the magnetic behaviors, meaning M and T_C values, which would limit its application potential in next-generation electronic devices.

Acknowledgments

This work has been funded by Vietnam National Foundation for Science and Technology Development (NAFOSTED) under grant number 103.02-2023.61.

Authors contributions

T. L. Phan, T. H. Nguyen: Methodology, Investigation, Manuscript writing, Supervision. H. T. Phuc, N. T. Dang, N. H. Tiep: Investigation, Formal analysis. P. D. Thang, H. N. Nhat: Formal analysis.

Conflict of interest

The authors have no conflict of interest to declare.

References

- [1] S. Wang, X. Liu and P. Zhou, The road for 2D semiconductors in the silicon age, Adv. Mater. 34 (2022) 2106886.
- [2] A. Hirohata, K. Yamada, Y. Nakatani, I.-L. Prejbeanu, B. Diény, P. Pirro, B. Hillebrands, *Review on spintronics: Principles and device applications*, J. Magn. Magn. Mater. **509** (2020) 166711.
- [3] S. A. Wolf, D. D. Awschalom, R. A. Buhrman, J. M. Daughton, S. von Molnár, M. L. Roukes *et al.*, *Spintronics:* A spin-based electronics vision for the future, Science **294** (2001) 1488.
- [4] I. Žutić, J. Fabian and S. Das Sarma, *Spintronics: Fundamentals and applications*, Rev. Mod. Phys. **76** (2004) 323.
- [5] A. K. Geim and K. S. Novoselov, The rise of graphene, Nat. Mater. 6 (2007) 183.
- [6] P. Huang, P. Zhang, S. Xu, H. Wang, X. Zhang and H. Zhang, Recent advances in two-dimensional ferromagnetism: materials synthesis, physical properties and device applications, Nanoscale. 12 (2020) 2309.
- [7] D. Joksas, A. AlMutairi, O. Lee, M. Cubukcu, A. Lombardo, H. Kurebayashi et al., Memristive, Spintronic, and 2D-materials-based devices to improve and complement computing hardware, Adv. Intell. Syst. 4 (2022) 2200068.
- [8] M. C. Lemme, D. Akinwande, C. Huyghebaert and C. Stampfer, 2D materials for future heterogeneous electronics, Nat. Commun. 13 (2022) 1392.
- [9] R. Ramesh, Materials for a sustainable microelectronics future: Electric field control of magnetism with multi-ferroics, J. Indian Inst. Sci. 102 (2022) 489.
- [10] S. Ning, H. Liu, J. Wu and F. Luo, Challenges and opportunities for spintronics based on spin orbit torque, Fundam. Res. 2 (2022) 535.
- [11] M. Schmitt, T. Denneulin, A. Kovács, T.G. Saunderson, P. Rüßmann, A. Shahee et al., Skyrmionic spin structures in layered Fe₅GeTe₂ up to room temperature, Commun. Phys. 5 (2022) 254.
- [12] K. Kim, J. Seo, E. Lee, K.-T. Ko, B.S. Kim, B.G. Jang et al., Large anomalous Hall current induced by topological nodal lines in a ferromagnetic van der Waals semimetal, Nat. Mater. 17 (2018) 794.
- [13] Q. Liu, J. Xing, Z. Jiang, Y. Guo, X. Jiang, Y. Qi et al., Layer-dependent magnetic phase diagram in Fe_nGeTe_2 (3 $\leq n \leq 7$) ultrathin films, Commun. Phys. 5 (2022) 140.
- [14] S. Albarakati, C. Tan, Z.-J. Chen, J.G. Partridge, G. Zheng, L. Farrar et al., Antisymmetric magnetoresistance in van der Waals Fe₃GeTe₂/graphite/Fe₃GeTe₂ trilayer heterostructures, Sci. Adv. 5 (2019) eaaw0409.
- [15] S. Ershadrad, S. Ghosh, D. Wang, Y. Kvashnin and B. Sanyal, *Unusual magnetic features in two-dimensional Fe*₅GeTe₂ induced by structural reconstructions, J. Phys. Chem. Lett. **13** (2022) 4877.
- [16] A.F. May, D. Ovchinnikov, Q. Zheng, R. Hermann, S. Calder, B. Huang et al., Ferromagnetism near room temperature in the cleavable van der Waals crystal Fe₅GeTe₂, ACS Nano. 13 (2019) 4436.
- [17] Y. Guo, Y. Zhao, S. Zhou and J. Zhao, Oxidation behavior of layered Fe_nGeTe₂ (n = 3, 4, 5) and Cr₂Ge₂Te₆ governed by interlayer coupling, Nanoscale. 14 (2022) 11452.
- [18] W. Xie, J. Zhang, Y. Bai, Y. Liu, H. Wang, P. Yu et al., Air stability and composition evolution in van der Waals Fe₃GeTe₂2,APL Mater. 12 (2024) 031102.

- [19] D. S. Kim, J. Y. Kee, J.-E. Lee, Y. Liu, Y. Kim, N. Kim et al., Surface oxidation in a van der Waals ferromagnet Fe_{3-x}GeTe₂, Curr. Appl. Phys. **30** (2021) 40.
- [20] T. Hu, Y. Ma, L. Lu, Y. Deng, M. Wang, K. Zhu et al., Enhanced magnetic transition temperature through ferromagnetic and antiferromagnetic interaction in cobalt-substituted Fe₅GeTe₂, Appl. Phys. Lett. 125 (2024) 022403.
- [21] A. F. May, C. A. Bridges and M. A. McGuire, Physical properties and thermal stability of Fe_{5-x}GeTe₂ single crystals, Phys. Rev. Mater. 3 (2019) 104401.
- [22] H. Wu, L. Chen, P. Malinowski, B. G. Jang, Q. Deng, K. Scott et al., Reversible non-volatile electronic switching in a near-room-temperature van der Waals ferromagnet, Nat. Commun. 15 (2024) 2739.
- [23] M. Joe, U. Yang and C. Lee, First-principles study of ferromagnetic metal Fe₅GeTe₂, Nano Mater. Sci. 1 (2019) 299.
- [24] E. Nshimyimana, X. Su, H. Xie, W. Liu, R. Deng, T. Luo et al., Realization of non-equilibrium process for high thermoelectric performance Sb-doped GeTe, Sci. Bull. 63 (2018) 717.
- [25] S. Kim, S. Yi Park, J. Jeong, G.-H. Kim, P. Rohani, D. Suk Kim et al., Production of pristine, sulfur-coated and silicon-alloyed germanium nanoparticles via laser pyrolysis, Nanotechnology 26 (2015) 305703.
- [26] A. Liu, X. Chen, Z. Zhang, Y. Jiang and C. Shi, Selective synthesis and magnetic properties of FeSe₂ and FeTe₂ nanocrystallites obtained through a hydrothermal co-reduction route, Solid State Commun. 138 (2006) 538.
- [27] P. D. Lodhi, N. Kaurav, K. K. Choudhary and Y. K. Kuo, Temperature-dependent transport properties of a FeTe compound, Bull. Mater. Sci. 42 (2019) 269.
- [28] D. H. Manh, T. D. Thanh, T. L. Phan and D. S. Yang, Towards hard-magnetic behavior of CoFe₂O₄ nanoparticles: a detailed study of crystalline and electronic structures, and magnetic properties, RSC Adv. 13 (2023) 8163.
- [29] T.-L. Phan, Y. D. Zhang, D. S. Yang, N. X. Nghia, T. D. Thanh and S. C. Yu, Defect-induced ferromagnetism in ZnO nanoparticles prepared by mechanical milling, Appl. Phys. Lett. 102 (2013) 072408.
- [30] G. Y. Khadzhai, A. L. Solovjov, M. V. Kislitsa, L. A. Paschenko, E. Nazarova, K. Buchkov et al., The effect of long-term exposure at room temperature on the thermal conductivity of the FeSe superconductor in the normal state, Low Temp. Phys. 49 (2023) 404.
- [31] C. Liu, B. A. Davidson, M. Zonno, S. Zhdanovich, R. Roemer, M. Michiardi et al., Protection of air-sensitive two-dimensional van der Waals thin film materials by capping and decapping process, Synchrotron Radiat. News. 36 (2023) 24.
- [32] K. Yi, Y. Wu, L. An, Y. Deng, R. Duan, J. Yang et al., Van der Waals encapsulation by ultrathin oxide for air-sensitive 2D materials, Adv. Mater. 36 (2024) 2403494.
- [33] J. Zhang, Z. Wang, Y. Xing, X. Luo, Z. Wang, G. Wang et al., Enhanced magnetic and electrical properties of Co-doped Fe₅GeTe₂, Appl. Phys. Lett. 124 (2024) 103103.
- [34] L. Liu, S. Chen, Z. Lin and X. Zhang, A symmetry-breaking phase in two-dimensional FeTe₂ with ferromagnetism above room temperature, J. Phys. Chem. Lett. 11 (2020) 7893.
- [35] P. Hu, T. Chang, W.-J. Chen, J. Deng, S.-L. Li, Y.-G. Zuo et al., Temperature effects on magnetic properties of Fe₃O₄ nanoparticles synthesized by the sol-gel explosion-assisted method, J. Alloys Compd. 773 (2019) 605.
- [36] L. Kang, C. Ye, X. Zhao, X. Zhou, J. Hu, Q. Li et al., Phase-controllable growth of ultrathin 2D magnetic FeTe crystals, Nat. Commun. 11 (2020) 3729.